

Graphene/Carbon Nanotubes Composite as a Polysulfide Trap for Lithium-Sulfur Batteries

Feng Gao^{1,2}, Xinxiu Yan^{1,2}, Zhikai Wei¹, Meizhen Qu¹, Weifeng Fan^{1,*}

¹ Chengdu Institute of Organic Chemistry, Chinese Academy of Sciences, Chengdu 610041, P.R. China.

² University of Chinese Academy of Sciences, Beijing 100049, P.R. China.

*E-mail: fanwf@cioc.ac.cn

Received: 12 December 2018 / Accepted: 17 January 2019 / Published: 10 March 2019

Separator modified with graphene/carbon nanotube composite (G/CNT) is introduced into lithium-sulfur (Li-S) battery to trap and activate the soluble polysulfides. The Li-S battery based on a novel separator allows sulfur cathode to reach a high initial discharge capacity of 1200 mAh.g⁻¹ at 0.2 C and a reversible capacity of 815 mAh.g⁻¹ after 100 cycles at 0.5 C, which led to an excellent rate capability (up to 2 C rate) and a high Coulombic efficiency of 99%. In this study, the role of separator modified with G/CNT in the electrochemistry of Li-S batteries was also systematically explored. The electrical conductivity and the special leaf stack structure of G/CNT layer have a synergistic effect in controlling the shuttle effect of polysulfides. Moreover, the G/CNT layer can compensate for the effects of deterioration of the morphology of sulfur cathode.

Keywords: Lithium-sulfur battery; Carbon nanotube; Graphene; Modified separator; Shuttle effect

1. INTRODUCTION

Solving environmental issues and achieving sustainable development are continuous in our society. In recent years, the rapid development of new energy sources provided favorable support for achieving those goals. However, all the new energy technologies, such as solar energy, wind energy, and tidal energy are the unstable energy sources. There should be a medium to store energy so that it can be released in a stable manner and the technology of storing energy is a key link in achieving sustainable development [1]. Lithium metal has come back into the agenda after nearly half a century of its silence. It is used as an anode to build lithium metal batteries with high energy density, owing to its low redox potential and high energy density [2-8]. Lithium-sulfur (Li-S) battery is one of the lithium-metal batteries [9-16], which due to the high energy density, low cost and environmental friendliness of sulfur, it has

been widely studied and is considered to be the closest commercialized lithium-metal battery. For a typical Li-S battery, it undergoes the following reaction: $16\text{Li} + \text{S}_8 \rightarrow 8\text{Li}_2\text{S}$. Unlike traditional lithium-ion batteries, Li-S battery undergoes a multielectron-transfer electrochemical process, where sulfur is lithiated from S_8 to Li_2S and a series of soluble intermediate i.e. Li_2S_x ($4 \leq x \leq 8$) is generated [10]. With the concentration gradient, the soluble Li_2S_x intermediate in the electrolyte diffuses from the positive to the negative electrode, and reacts with the lithium metal directly, resulting in a continuous loss of active sulfur and lithium metal, making Li-S battery suffering from low Coulombic efficiency and poor cycle performance. This is referred as shuttle effect and is the main obstacle to the commercialization of Li-S battery.

In order to overcome this problem, tremendous efforts have been made to improve the electrochemical performance of Li-S battery. In recent years, many scientists focus on the modified separator [17-19]. Modifying the separator with a carbon layer has been proved to be an effective method to improve the performance of Li-S battery [20, 21]. Graphene, with its special two-dimensional (D) planar structure and excellent electrical conduction, it is often used to improve the cycle performance of Li-S batteries [22-24]. However, the layers of graphene usually stack severely, which seriously reduces the efficiency of its action on sulfur. Recently, 3D composites containing 2D graphene and 1D carbon nanotubes (CNTs) have emerged as interlayers between sulfur cathodes and separator to trap polysulfides owing to their micro/mesoporous architectures [25, 26]. However, the reported graphene/CNT composite is synthesized by growing CNTs on graphene with Fe/Ni catalyst. The impurities of the reported graphene/CNT composite can affect the function of highly open structure of G/CNT in Li-S batteries. The processing complexity, low productivity, and agglomerated morphologies in G/CNT have also limited their applications. In addition, finding out the reason for this highly porous and loose structure which effectively suppresses the shuttle effect is also worthy of study.

On this context, in this study a separator modified with graphene/CNT (G/CNT) with a high conductivity (G/CNT mass load of 0.176 mg.cm^{-2}) was prepared. The G/CNT was prepared by a simple method which could be applied for large-scale production and has no catalyst in the G/CNT composites. Moreover, the role of the loose structure of G/CNT modified layer on the separator in the electrochemistry of Li-S batteries has been systematically explored.

2. EXPERIMENTAL

2.1. Preparation of G/CNT

G/CNT was purchased from Timesnano Inc., China. graphene oxide (Chengdu Organic Chemicals Co. Ltd., Chinese Academy of Sciences) and carbon nanotube powder (Chengdu Organic Chemicals Co. Ltd., Chinese Academy of Sciences) at a weight ratio of 1:1 were mixed and made into a slurry. Then, a specific amount of surfactant was added into the above solution. Following this, binder and curing agent were added to form the precursor solution. This solution was then evaporated to dryness and subjected to a curing treatment to obtain a composite powder of graphene and carbon nanotubes (G/CNT). This powder was subsequently calcined at 1200°C in N_2 atm.

2.2. Preparation of G/CNT coated separator

G/CNT slurry was obtained by mixing 90 wt% G/CNT powder and 10 wt% LA133 in $(\text{CH}_3)_2\text{CHOH}/\text{H}_2\text{O}$ (3:1, vol) and milled at 350 rpm for 5 h. The solid content of slurry is about 3%. Subsequently, the obtained slurry was coated on one side of a Celgard PP separator (25 μm thick) with a doctor blade. Then, the separator coated with slurry was dried in a vacuum oven at 60 °C for 5 h. Finally, G/CNT coated separator was punched into a disk with a diameter of 19 mm for assembling the cells.

2.3. Preparation of sulfur cathode

Using the conventional method the sulfur cathode was prepared. The sulfur/carbon composite was obtained by mixing sulfur powder and G/CNT at a weight ratio of 3:1, and then heated at 155 °C for 12 h in Ar atm. The slurry was prepared by mixing 90 wt% sulfur/carbon composite and 10 wt% LA133 in $(\text{CH}_3)_2\text{CHOH}/\text{H}_2\text{O}$ (3:1, vol) and milled at 350 rpm for 5 h. The slurry was spread on the aluminum substrate by a doctor blade and dried in a vacuum oven at 60 °C for 5 h. The sulfur mass loads in the cathode are 1.7-2 mg cm^{-2} .

2.4. Electrochemistry Measurements

In order to evaluate the electrochemical performance of Li-S battery, 2032 type coin cells were assembled using lithium metal as the counter/reference electrode and Celgard 2500 as a separator. The electrolyte consisted of a solution of 1 M LiTFSI in 1,3-dioxolane (DOL) and 1,2-dimethoxyethane (DME) (1:1, vol) with 2 wt% LiNO₃. Galvanostatic charge/discharge measurements were performed on a NEWARE (BTS-5V 10 mA) system in the voltage ranges of 1.7-2.8 V (vs. Li⁺/Li). Electrochemical impedance spectroscopy (EIS) data were collected using Autolab multichannel electrochemical workstation (Metrohm, Multi Autolab/M204). The frequency ranges were from 100 kHz to 10 mHz with an AC voltage amplitude of 5 mV.

2.5. Characterization

The characterization on the morphology and structure of the obtained materials were carried out via scanning electron microscopy (SEM, INCA Pen-taFETx3) equipped with energy dispersive X-ray spectroscopy (EDS, Oxford X-Max). The Brunauer-Emmett-Teller (BET) specific surface area and pore-size distribution (from the adsorption branches of the isotherms) were determined by nitrogen adsorption/desorption isotherm curves using a Micromeritics ASAP 2020 system.

3. RESULTS AND DISCUSSION

3.1. Configuration and Characterization of the G/CNT coated Separator

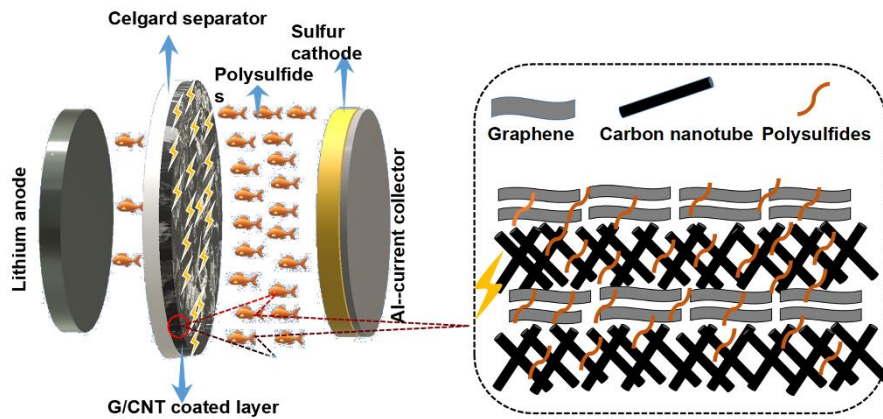


Figure 1. The schematic of the configuration of Li-S battery with a G-CNT modified separator.

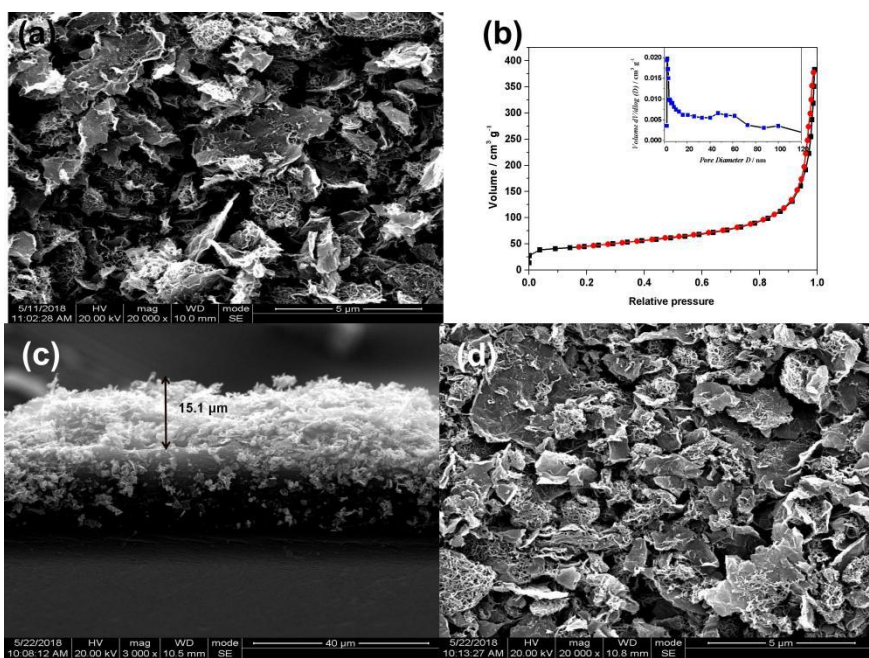


Figure 2. G/CNT composite (a) SEM image and (b) Nitrogen adsorption-desorption isotherm plots. Inset: the pore-size distribution of G/CNT composite; G/CNT modified separator (c) side view and (d) top view.

Figure 1 presents the polypropylene separator consisting of a lightweight and conductive G/CNT coating on its one side which faces sulfur cathode. G/CNT coated layer of the separator acts as a barrier and also serves as a conductive layer along with functioning as an “upper” current collector [27]. As

depicted in Figure 1, G/CNT coated layer impedes the migration of polysulfides thereby preventing them from diffusing through the separator. Figure 2a shows SEM image of G/CNT composite whereby the formation of an integrated 3D structure of graphene and CNT could be noted by following a simple strategy. This highly open and loose structure promises the penetration and circulation of electrolyte and also lithium ions can easily transport through the coated separator [28]. As illustrated in Figure 2b, nitrogen adsorption-desorption isotherms together with the pore-size distribution were measured to obtain the specific surface area and the pore structure of G/CNT composite. The BET specific surface area of G/CNT composite is $153 \text{ m}^2 \cdot \text{g}^{-1}$ which demonstrates that the complex contains a limited pore volume. Combining with the SEM image, a large number of holes in G/CNT could be considered belonging to macropores. Moreover, it still maintains the same structure after coating G/CNT composite on the separator (Figures 2c and 2d). The complex 3D structure and large specific surface area of G/CNT can increase the chances of contact with polysulfides in G/CNT, and suppress the diffusion of polysulfides [27, 29]. It is to be noted that the loading of G/CNT composite on the separator is approximately $0.17 \text{ mg} \cdot \text{cm}^{-2}$, which is much lighter than Celgard separator ($1.1 \text{ mg} \cdot \text{cm}^{-2}$).

3.2. Electrochemical Analyses of Sulfur Cathode Utilizing the G/CNT coated Separator

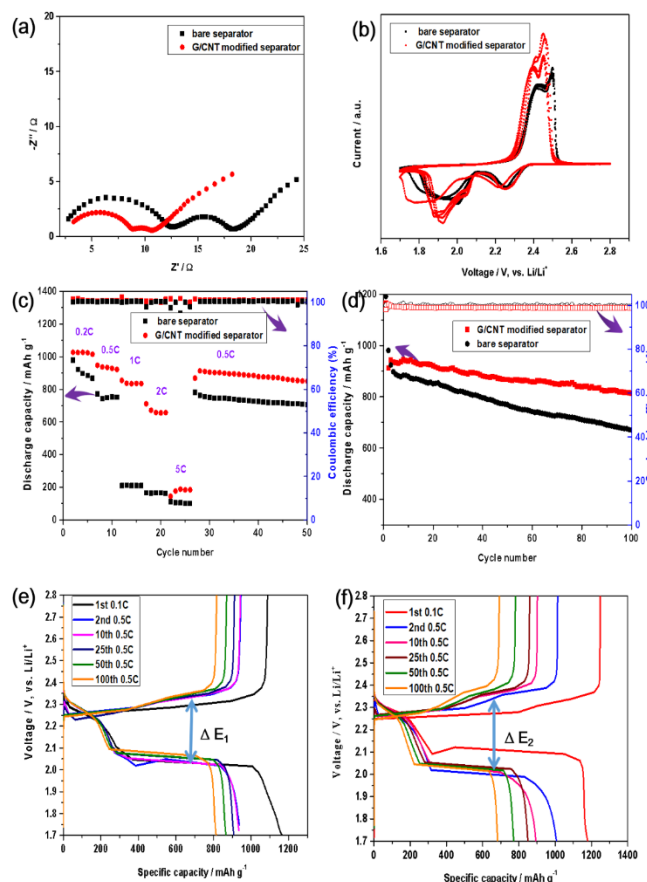


Figure 3. (a) EIS (after 100 cycles) and (b) CV curves of Li-S battery; (c) Rate performance and (d) Cycle performance of Li-S battery in 0.5 C; The charge-discharge curves of Li-S battery with (e) G/CNT modified separator and (f) bare separator.

The EIS of the batteries were measured to characterize the resistance of Li-S battery with G/CNT coated separator and bare separator after 100 cycles (Figure 4a). The open circuit voltages for both the batteries were at 2.4 V. Both the impedance spectra exhibited two depressed semicircles in high and medium frequency regions followed by an inclined line indicating the solid-state. It is believed that the semicircle in the high-frequency region reflecting the charge-transfer process at carbon interface (R_{ct}) and the semicircle in the medium frequency region could be related to the formation of solid films of $\text{Li}_2\text{S}_2/\text{Li}_2\text{S}$ on the cathode surface (R_{sei}) [30-32]. It could be seen that both R_{ct} and R_{sei} are significantly reduced, which is in agreement with previous observations [28]. They can be ascribed to the integral 3D framework of G/CNT which holds polysulfides and facilitating the transfer of electrons and diffusion of ions.

Figure 3b shows CV curves of Li-S batteries with G/CNT coated separator and bare separator. The CV curves of battery with bare separator measured in the first five cycles present two typical oxidation peaks centered at ~ 2.42 V and ~ 2.49 V, and two typical reduction peaks at ~ 2.26 V and ~ 2.01 V [33]. Compared to the battery with bare separator, the battery with G/CNT coating demonstrated a decrease in the oxidation peak (~ 2.39 V and ~ 2.44 V) and a sharp reduction peak (~ 2.26 V and ~ 2.05 V). It shows that G/CNT coating can enhance the electrochemical kinetics and decrease the cell polarization [28]. The results obtained from CV agree well with EIS.

The rate performance of G/CNT modified battery has been further studied as shown in Figure 3c. When the current increased to 1 C, it could still deliver a reversible capacity of 836 mAh.g^{-1} . Even at very high rates of 2 C, the electrode retained a specific capacity of 655 mAh.g^{-1} . However, the battery with bare separator shows poor rate performance. Figure 3d shows the cycling stability of batteries with different separators. Compared to the rapid decay in capacity to 670 mAh.g^{-1} within 100 cycles of battery with bare separator, the battery with G/CNT modified separator exhibits a capacity of 813 mAh.g^{-1} after 100 cycles, corresponding to a retention rate of 89%, which is much higher than 67% of battery with bare separator (calculated from 2nd cycle). It can be ascribed to the upper collective conductive effect of G/CNT coating [34].

The galvanostatic discharge-charge curves of Li-S battery with different separators at 0.5 C are shown in Figures 3e and 3f. Two batteries exhibit typical voltage profiles with two main discharge plateaus at around 2.3 V and 2.0 V, which is consistent with the results of CV. Also, Li-S battery with bare separator is more severely polarized than G/CNT modified separator ($\Delta E_1 < \Delta E_2$). As shown in Figure 4f, it could be observed that overcharging of the initial charge-discharge curve of Li-S batteries is serious, which can be attributed to the well-known shuttle effect of Li-S batteries [35, 36]. Conversely, the shuttle effect of Li-S batteries with G/CNT modified separator is well suppressed. This also indicates that G/CNT modified separator can capture the polysulfide dissolved in the electrolyte.

3.3 Morphological and Elemental Mapping Analyses of the Cycled G/CNT coated Separator

Figures 4a and 4b show the morphology of G/CNT coating layer after 100 cycles. A large number of particles, believed to be sulfur particles, adhere to the G/CNT skeleton after cycling could be seen. Polysulfides that diffuse from cathode are captured by G/CNT on the separator [37]. Figures 4c and 4d

show the elemental distribution of sulfur and carbon on the G/CNT coating layer (top view), respectively. The uniform distribution of sulfur on the surface of G/CNT coating could be noted. These results indicate that G/CNT coating does have a beneficial effect on the capture of sulfur species.

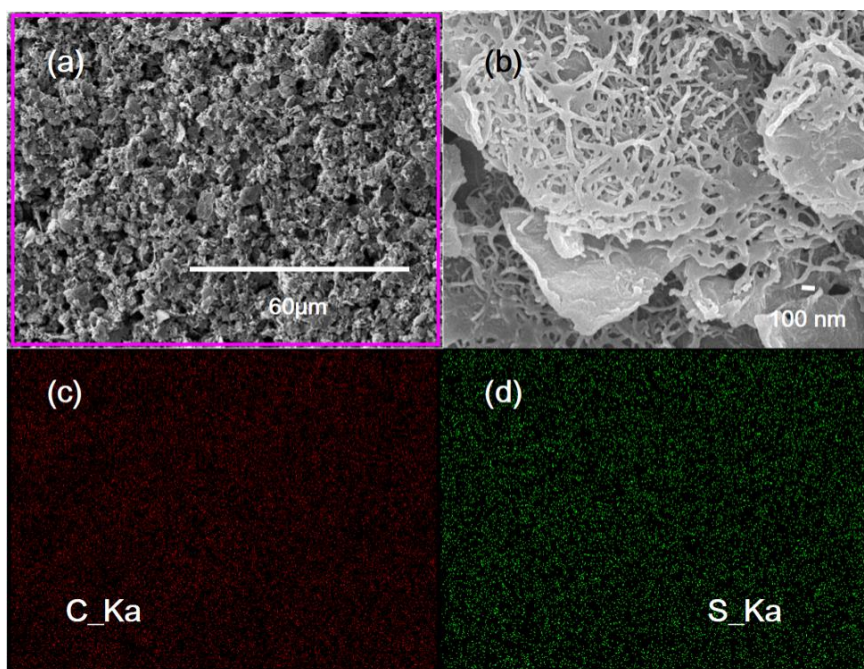


Figure 4. (a, b) SEM image of G/CNT coating on the separator after 100 cycles in 0.5 C; EDS images of corresponding elemental mapping of (c) carbon and (d) sulfur.

3.4 Elemental Analyses of the Surface of Cycled Lithium Anode

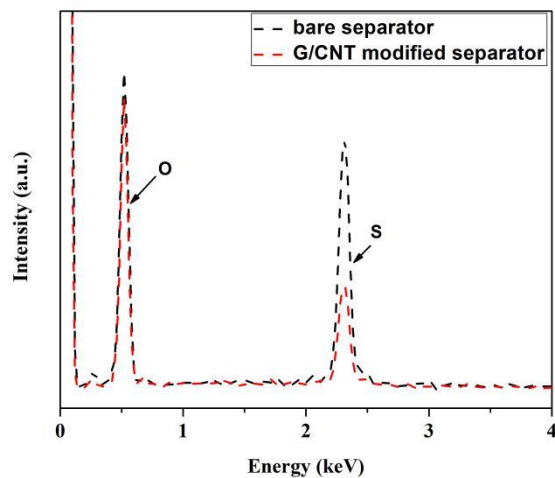


Figure 5. EDS spectrum of the surface of lithium anode of Li-S battery with bare separator and G/CNT separator.

Figure 5 shows the relative content of sulfur and oxygen on the surface of lithium metal after 100 cycles. Both the surface of lithium anode of batteries with bare separator and G/CNT modified separator containing oxygen and sulfur elements could be noticed. The appearance of oxygen may be caused by the decomposition of electrolyte and the oxidation of lithium by air, whereas the sulfur peak is caused by the diffusion of polysulfide from the cathode [38- 40]. Moreover, the relative content of sulfur in the battery with bare separator is 13.93%, which is almost doubled for the G/CNT coated one (8.56%). This outcome strongly suggests that G/CNT can effectively inhibit the diffusion of polysulfide, which is consistent with the results already reported in the literature [37].

3.4 What factors actually work

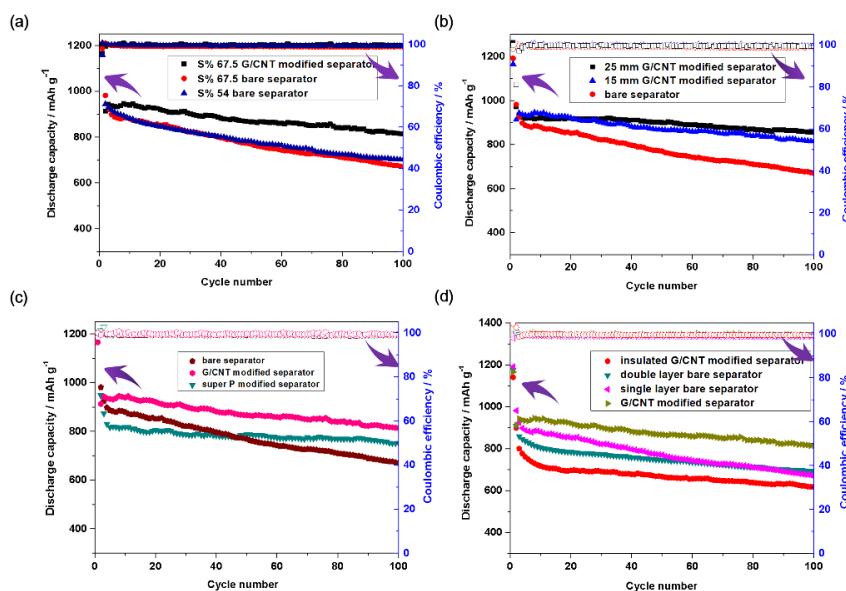


Figure 6. (a) Cycle performance of Li-S battery with different S contents; (b) Cycle performance of Li-S battery with different interlayers; (c) Cycle performance of Li-S battery with Super P and G/CNT modified separator; (d) Cycle performance of Li-S battery with separator modified with different thickness of G/CNT layers.

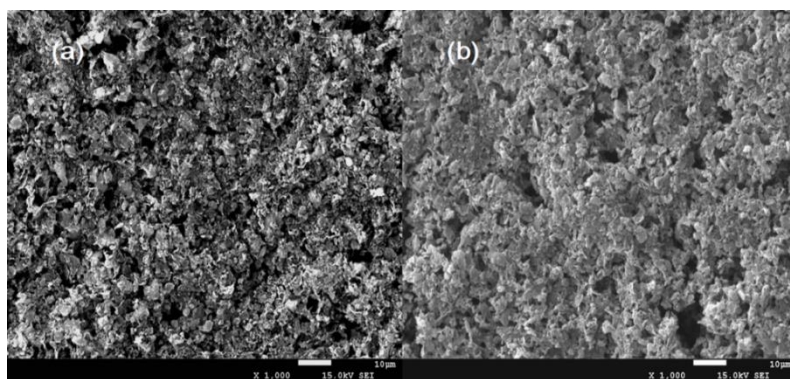


Figure 7. The surface morphology of sulfur cathode (a) before and (b) after 100 cycles.

In order to gain a better understanding on the mechanism of action of G/CNT layer in Li-S batteries, series of experiments were carried out to verify whether the noted facts are in accordance with what have been predicted in Figure 1.

Sulfur Content The first factor that was excluded is the effect of sulfur/carbon ratio on the battery. If the carbon in the G/CNT modified separator is included in the calculations, the sulfur content of whole battery will be reduced from 67.5 to 54%. However, reducing the sulfur/carbon ratio may impact the performance of Li-S battery [37, 42, 43] and thus the influence of this factor could be excluded. Based on this, the sulfur content was reduced to 54% to test the cycle performance of Li-S battery and the obtained results are shown in Figure 6a. It could be seen that, reducing the sulfur content does not effectively improve the cycle performance of Li-S battery. Figure S1 displays the EIS of Li-S battery with a S content of 54%. Although the sulfur content is reduced, the polarization during charging and discharging is still quite large. Therefore, it is assumed that the improvement of cycle performance of Li-S battery with G/CNT modified separator is not caused by simply reducing the sulfur content.

Structure of G/CNT As shown in Figure 6b, the thickness of G/CNT layer was increased and the cycle performance of Li-S battery with G/CNT of 15 μm and 25 μm modified separator (SEM image is shown in Figure S2) was tested. From Figure 6b, it is prominent that increasing the thickness of G/CNT layer can improve the utilization of sulfur and reduce the decay in the cycle capacity of Li-S battery as reported earlier [31, 43]. Figure S3 shows the EIS of Li-S batteries with 15 μm and 25 μm G/CNT modified separator. With an increase in the thickness of G/CNT layer, R_{ct} further reduces but there is no significant change in R_{sei} . As illustrated in Figure 5c, the separator was then coated with the same mass loads of Super P and the battery for the cycle performance was tested. Figure S4 shows the nitrogen adsorption-desorption isotherm plots of Super P and the inset figure is the pore-size distribution of Super P powder. The BET specific surface area of Super P powder is 61.2 $\text{m}^2 \text{ g}^{-1}$ and it contains a limited amount of micropores and mesopores. Figure S5 shows the SEM images of (a) Super P powder and (b, c) Super P coated separator. The particle size of Super P does not exceed 80 nm and the coated layer is only 4.16 μm . However, the mass load of Super P is 0.156 mg.cm^{-2} , which is same as that of G/CNT coated layer. It indicates that the density of G/CNT is much smaller than that of super P. It also denotes that G/CNT coating is thicker with the same quality of Super P, which is more conducive to the capture of polysulfide. Since Super P has a high specific surface area and excellent electrical conductivity [45, 46], it can also play a major role in trapping polysulfides dissolved in the electrolyte which is beneficial to the cycle stability of Li-S battery [47]. However, it does have a limited specific surface area. Figure S6 shows the EIS of Li-S battery with Super P modified separator which presents a significant improvement in the attenuation capacity, but without any enhancements in the utilization rate of sulfur. This outcome illustrates that G/CNT with a high specific surface area and complex 3D structure is more effective in trapping polysulfide and increasing the utilization of sulfur.

Conductivity of G/CNT interlayer Subsequently, a bare separator was added between G/CNT layer and cathode to make G/CNT layer electrically insulated. By this, whether the conductivity of G/CNT layer plays a role in improving the performance of Li-S battery could be verified. Also, Li-S battery with a double-layer bare separator was used (as a blank experiment) to rule out the effect of applying an extra bare separator on the performance of battery. The cycle performance of Li-S battery is shown in Figure 6d, and it could be observed that employing a double-layered bare separator does not

have a significant effect on the cycle stability of battery, whereas using G/CNT modified separator which loses its conductivity produces a significant negative effect on the long-cycle performance of Li-S battery. Obviously, the utilization rate of sulfur is significantly lower which may be due to that G/CNT layer with a high specific surface area confines polysulfides effectively in the G/CNT layer [21]. The trapped polysulfides cannot be utilized to produce dead sulfur, resulting in a decrease in the utilization of sulfur in the entire Li-S battery and a decline in the cycle performance [37, 47]. It suggests that the electrical conductivity of G/CNT layer is a key factor in controlling the shuttle effect of polysulfides.

Evolution on the structure of cathode In the preparation of sulfur cathode, solid-state sulfur and carbon are thermally recombined. Solid sulfur plays a certain structural support before cycling, while it undergoes a phase change from solid to liquid during charging and discharging. The transformation will have a huge impact on the structure of cathode [31, 43]. Figure 7 shows the morphology of sulfur cathode before and after 100 cycles. It could be found that the surface of cathode was relatively flat and intact before cycling. Whereas after 100 cycles, a large number of holes appearing on the surface of sulfur electrode. These holes cause sulfur or polysulfides in the sulfur cathode to lose the protection of carbon material. Sulfur or polysulfides in the sulfur cathode directly exposed to lithium anode, and diffusing out cathode without any barriers [47]. The G/CNT layer built on the separator has no sulfur which is not easy to lose its structure. Sulfur does not support the skeleton and the structure is relatively stable [43]. So, it can capture and block the diffused polysulfides effectively and permanently as a secondary capture network.

4. CONCLUSION

In summary, G/CNT modified separator is introduced in Li-S batteries to trap and activate the soluble polysulfides. As a result, the G/CNT coated separator allows sulfur cathode to reach a high initial discharge capacity of 1200 mAh.g^{-1} at 0.2 C and a reversible capacity of 815 mAh.g^{-1} after 100 cycles at 0.5 C, and led to an excellent rate capability (up to 2 C rate) and a high Coulombic efficiency of 99%, which is higher than the battery with bare separator. The excellent electrochemical performance of Li-S battery with G/CNT modified separator can be attributed to the presence of G/CNT layer, which can capture and activate polysulfides effectively. Both the electrical conductivity and complex 3D structure of G/CNT layer have a synergistic effect in controlling the shuttle effect of polysulfide. Moreover, the G/CNT layer can compensate for the effects of deterioration of the morphology of sulfur cathode. Thus, a simple method has been followed to prepare G/CNT material and was then employed to modify the Li-S battery separator, which in turn greatly improved the performance of Li-S battery. The modified Li-S battery separator is expected to have great application prospects in the field of Li-S batteries.

ACKNOWLEDGEMENTS

Authors would like to thank National Natural Science Foundation of China (grant no.51474196) and Sichuan Provincial Department of Science and Technology Project (grant no. 2017GZ0114).

SUPPORTING INFORMATION

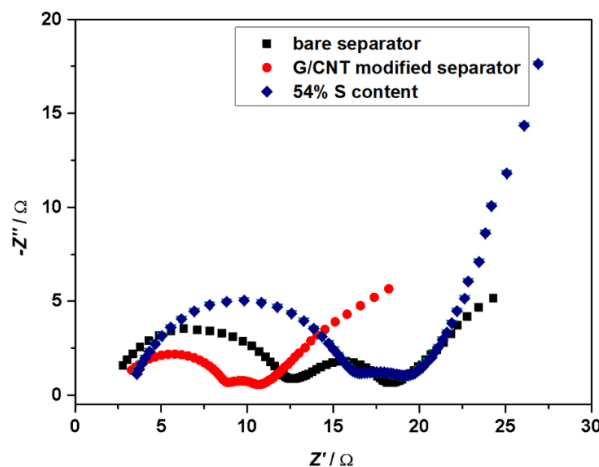


Figure S1. EIS of Li-S battery with 54% sulfur content of sulfur cathode.

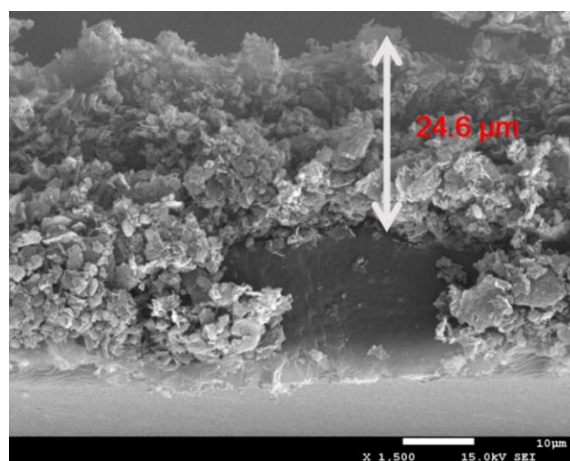


Figure S2. SEM image of 25 μm G/CNT modified separator (side view).

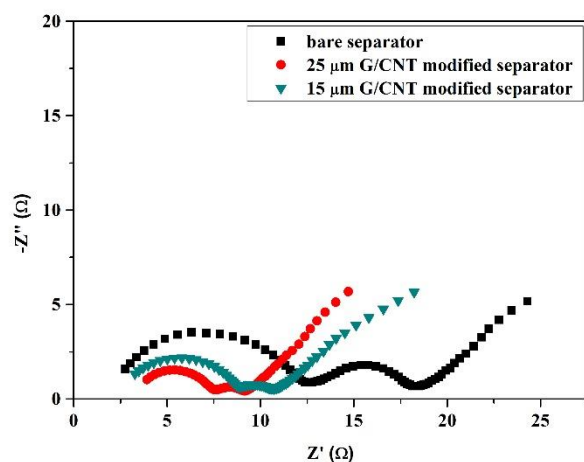


Figure S3. EIS of Li-S battery with 25 μm and 15 μm G/CNT-modified separator.

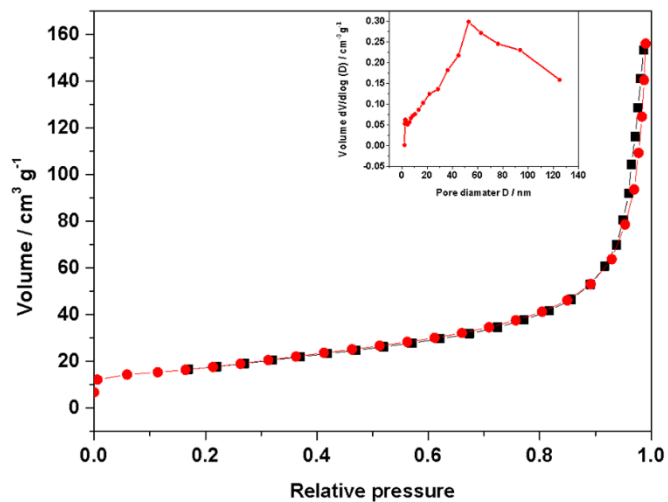


Figure S4. Nitrogen adsorption-desorption isotherms plot of super P. Inset: the pore-size distribution of super P powder.

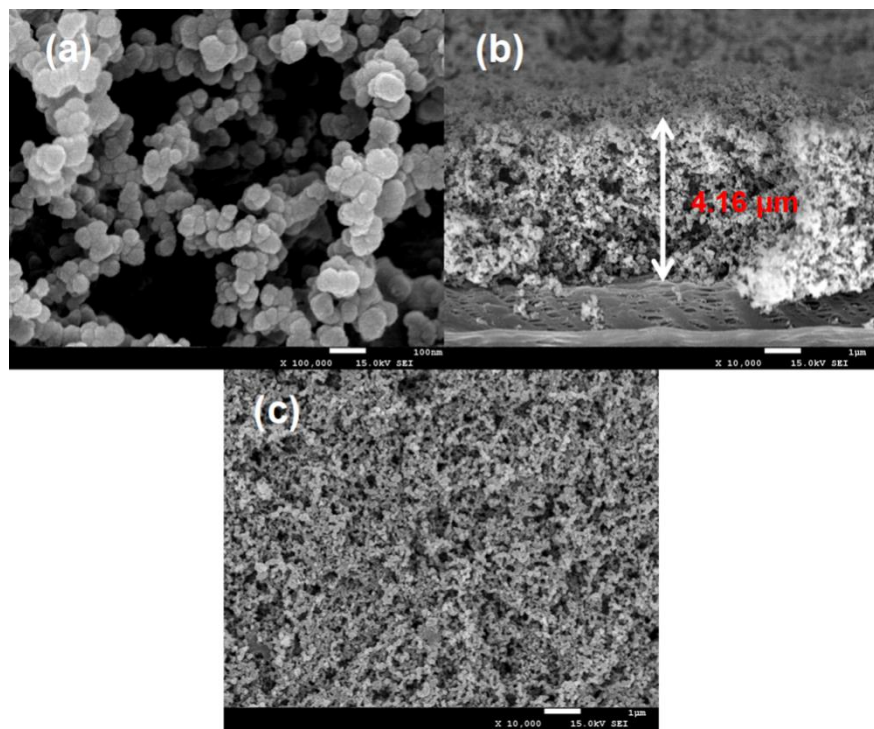


Figure S5. SEM images of (a) super P powder, (b) side view and (c) top view of super P modified separator.

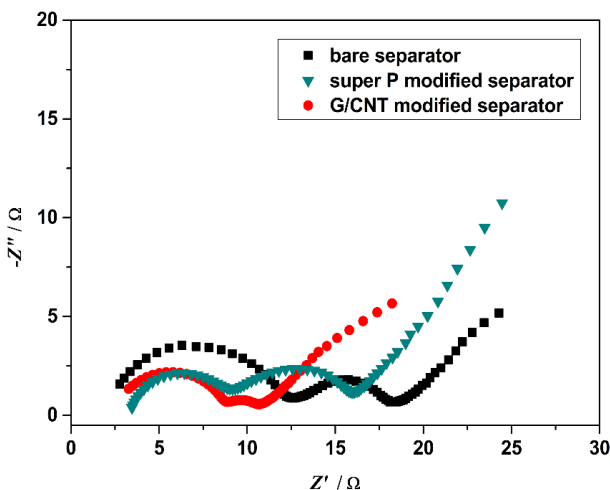


Figure S6. EIS of Li-S battery with super P modified separator.

References

1. M. Armand and J.M. Tarascon, *Nature*, 451 (2008) 652.
2. J.M. Tarascon and M. Armand, *Nature*, 414 (2001) 359.
3. P. Poizot, S. Laruelle, S. Grugeon, L. Dupont and J.M. Tarascon, *Nature*, 407 (2000) 496.
4. P.G. Bruce, B. Scrosati and J.M. Tarascon, *Angew. Chem. Int. Edit.*, 47 (2008) 2930.
5. M.S. Whittingham, *Chem. Rev.*, 104 (2004) 4271.
6. K. Xu, *Chem. Rev.*, 104 (2004) 4303.
7. B. Scrosati and J. Garche, *J. Power Sources*, 195 (2010) 2419.
8. G. Girishkumar, B. McCloskey, A.C. Luntz, S. Swanson and W. Wilcke, *J. Phys. Chem. Lett.*, 1 (2010) 2193.
9. A. Manthiram, Y. Fu, S.H. Chung, C. Zu and Y.S. Su, *Chem. Rev.*, 114 (2014) 11751.
10. Y.V. Mikhaylik and J.R. Akridge, *J. Electrochem. Soc.*, 151 (2004) A1969.
11. Y.X. Yin, S. Xin, Y.G. Guo and L.J. Wan, *Angew. Chem. Int. Edit.*, 52 (2013) 13186.
12. A. Manthiram, Y. Fu and Y.S. Su, *Accounts Chem. Res.*, 46 (2013) 1125.
13. S.S. Zhang, *J. Power Sources*, 231 (2013) 153.
14. G. Zhou, F. Li and H.M. Cheng, *Energy Environ. Sci.*, 7 (2014) 1307.
15. A. Manthiram, S.H. Chung and C. Zu, *Adv. Mater.*, 27 (2015) 1980.
16. D. Zheng, X.Q. Yang and D. Qu, *ChemSusChem*, 9 (2016) 2348.
17. J. Huang, Y. Sun, Y. Wang and Q. Zhang, *Acta Chimica Sinica*, 75 (2017) 173.
18. Y. Xiang, J. Li, J. Lei, D. Liu, Z. Xie, D. Qu, K. Li, T. Deng and H. Tang, *ChemSusChem*, 9 (2016) 3023.
19. N. Deng, W. Kang, Y. Liu, J. Ju, D. Wu, L. Li, B.S. Hassan and B. Cheng, *J. Power Sources*, 331 (2016) 132.
20. S.H. Chung and A. Manthiram, *Adv. Funct. Mater.*, 24 (2014) 5299.
21. H. Yao, K. Yan, W. Li, G. Zheng, D. Kong, Z.W. Seh, V.K. Narasimhan, Z. Liang and Y. Cui, *Energy Environ. Sci.*, 7 (2014) 3381.
22. K. Chen, Z. Sun, R. Fang, F. Li, and H. Cheng, *Acta Physico-Chimica Sinica*, 34 (2018) 377.
23. L. Zhang, F. Wan, X. Wang, H. Cao, X. Dai, Z. Niu, Y. Wang and J. Chen, *ACS Appl. Mater. Interfaces*, 10 (2018) 5594.
24. Y. Liu, X. Qin, S. Zhang, G. Liang, F. Kang, G. Chen and B. Li, *ACS Appl. Mater. Interfaces*, 10 (2018) 26264.

25. H.W. Wu, Y. Huang, W.C. Zhang, X. Sun, Y.W. Yang, L. Wang and M. Zong, *J. Alloy. Compd.*, 708 (2017) 743.
26. G.G. Kumar, S.H. Chung, T.R. Kumar and A. Manthiram, *ACS Appl. Mater. Interfaces*, 10 (2018) 20627.
27. H. Wu, Y. Huang, W. Zhang, X. Sun, Y. Yang, L. Wang and M. Zong, *J. Alloys Compd.*, 708 (2017) 743.
28. J. Deng, J. Li, J. Guo, M. Zeng, D. Zhao and X. Yang, *Int. J. Electrochem. Sci.*, 13 (2018) 3651.
29. M.Q. Zhao, X.F. Liu, Q. Zhang, G.L. Tian, J.Q. Huang, W. Zhu and F. Wei, *ACS Nano*, 6 (2012) 10759.
30. J. Sun, Y. Sun, M. Pasta, G. Zhou, Y. Li, W. Liu, F. Xiong and Y. Cui, *Adv. Mater.*, 28 (2016) 9797.
31. J. Yan, X. Liu and B. Li, *Adv. Sci.*, 3 (2016) 1600101.
32. L. Wang, J. Zhao, X. He and C. Wan, *Electrochim Acta*, 56 (2011) 5252.
33. Y.S. Su and A. Manthiram, *Electrochim Acta*, 77 (2012) 272.
34. B.B. Zheng, L.W. Yu, Y. Zhao and J.Y. Xi, *Electrochim. Acta*, 295 (2019) 910.
35. N. Xu, T. Qian, X. Liu, J. Liu, Y. Chen, and C. Yan, *Nano Lett.*, 17 (2017) 538.
36. A.F Hofmann, D.N Fronczek and W.G Bessler, *J. Power Sources*, 259 (2014) 300.
37. C.H. Chang, S.H. Chung and A. Manthiram, *Small*, 12 (2016) 174.
38. D. Aurbach, E. Pollak, R. Elazari, G. Salitra, C.S. Kelley and J. Affinito, *J. Electrochem. Soc.*, 156 (2009) A694.
39. X. Chen, T.Z. Hou, B. Li, C. Yan, L. Zhu, C. Guan, X.B. Cheng, H.J. Peng, J.Q. Huang and Q. Zhang, *Energy Storage Materials*, 8 (2017) 194.
40. S. Xiong, K. Xie, Y. Diao and X. Hong, *J. Power Sources*, 246 (2014) 840.
41. M. Chen, S. Jiang, C. Huang, J. Xia, X. Wang, K. Xiang, P. Zeng, Y. Zhang and S. Jamil, *ACS Appl. Mater. Interfaces*, 10 (2018) 13562.
42. R. Chulliyote, H. Hareendrakrishnakumar, M. Raja, J.M. Gladis and A.M. Stephan, *Chemistryselect*, 2 (2017) 10484.
43. S.H. Chung and A. Manthiram, *Chem. Commun.*, 50 (2014) 4184.
44. H. Yao, K. Yan, W. Li, G. Zheng, D. Kong, Z. Seh, V. K. Narasimhan, Z. Liang and Y. Cui, *Energy Environ. Sci.*, 7 (2014) 3381.
45. R.M. Gnanamuthu and C.W. Lee, *Mater. Chem. Phys.*, 130 (2011) 831.
46. I. Cho, J. Choi, K. Kim, M.H. Ryou and Y.M. Lee, *RSC Adv.*, 115 (2015) 95073.
47. N.I. Kim, C.B. Lee, J.M. Seo, W.J. Lee and Y.B. Roh, *J. Power Sources*, 132 (2004) 209.